Synthesis, Isolation, and Spectroscopic Characterization of Holmium–Based Mixed-Metal Nitride Clusterfullerenes: HoxSc3–xN@C80 (x=1, 2)

ARTICLE *in* CHEMISTRY - A EUROPEAN JOURNAL · JULY 2012

Impact Factor: 5.73 · DOI: 10.1002/chem.201200574 · Source: PubMed

4 AUTHORS, INCLUDING:

Alexey A Popov
Leibniz Institute for Solid State and Materia…
188 PUBLICATIONS **3,410** CITATIONS

SEE PROFILE

CHEMISTRY
A EUROPEAN JOURNAL

FULL PAPER

DOI: 10.1002/chem.200((will be filled in by the editorial staff))

Synthesis, Isolation and Spectroscopic Characterization of Holmium-Based Mixed Metal Nitride Clusterfullerenes: $Ho_xSc_{3-x}N@C_{80}$ (x=1, 2)

Yang Zhang, Alexey A Popov, Sandra Schiemenz, and Lothar Dunsch*

Abstract: The synthesis, isolation and spectroscopic characterization of $Ho_xSc_{3-x}N@C_{80}$ (x=1, 2) is reported. Two isomers of Holmium-based mixed metal nitride clusterfullerenes, $Ho_xSc_{3-x}N@C_{80}$ (x=1, 2), have been synthesized by "reactive gas atmosphere" method and isolated by multi-step recycling HPLC. The isomeric structures of $Ho_xSc_{3-x}N@C_{80}$ (x=1, 2) were characterized by laser-desorption time-of-flight (LD-TOF) mass spectroscopy, UV-Vis-NIR, FTIR and Raman spectroscopy. A comparative study of $M_xSc_{3-x}N@C_{80}$ (M= Gd, Dy, Lu, and Ho) demonstrates the dependence of their electronic and vibrational properties on the encaged metal. Despite the distinct perturbation induced by $4f^{10}$-electrons, we report the first paramagnetic ^{13}C NMR study on $Ho_xSc_{3-x}N@C_{80}$ (I; x= 1, 2) and confirm I_h-symmetric cage structure. The ^{45}Sc NMR study of $HoSc_2N@C_{80}$ (I, II) exhibits a temperature-dependent chemical shift in the temperature range of 268-308 K.

Keywords: fullerenes • synthesis and isolation • ^{13}C NMR • ^{45}Sc NMR • paramagnetic NMR • vibrational spectroscopy

Introduction

Soon after the discovery of $Sc_3N@C_{80}$ in 1999,[1] one of the directions in which nitride clusterfullerenes research branched was the study of mixed metal nitride clusterfullerenes (MMNCFs) with two or three different metals in the nitride cluster. Numerous C_{80}-based MMNCFs have been successfully isolated and characterized over the last decade, including $MSc_2N@C_{80}$ (I, M= Ti,[2] Y,[3] Ce,[4] Nd,[5] Dy,[5] Tb,[6] and Er[7]), $M_2ScN@C_{80}$ (I, M= Y,[3] Nd,[5] Dy,[5] and Er[8, 9]), $ScYErN@C_{80}$,[10] $Gd_xSc_{3-x}N@C_{80}$ (I, II; x=1, 2),[6, 11, 12] $Lu_xSc_{3-x}N@C_{80}$ (I, II; x=1, 2)[5] and $Lu_xY_{3-x}N@C_{80}$ (I, x=1, 2).[13] Furthermore, the feasibility of varying the encapsulated metal atoms, stabilizing different cage sizes (i.e. $Lu_xSc_{3-x}N@C_{68}$ (x=1, 2),[14] $DySc_2N@C_{68}$,[14] and $DySc_2N@C_{76}$[15]) and the existence of different isomeric structures are believed to give rise to special electrochemical,[3, 10, 16] optical[17] and magnetic properties of MMNCFs.[18]

^{13}C NMR spectrometry is one of the most important tools for the structure elucidation of fullerenes. Continuous efforts have been dedicated to attaining the ^{13}C NMR data from the Scandium-, Yttrium- and Lutetium-based homogeneous and MMNCFs.[1, 5, 13, 19] Furthermore, π-orbital axis vector (POAV) analysis together with experimental ^{13}C NMR studies showed that the enlargement of the size of encaged metal nitride clusters enhances the local curvature of the carbon cage in the vicinity of metal atoms.[13] Taking into the account the paramagnetic contribution of the 4f-electrons from the encaged metals, among the existing of homogenous metal nitride NCFs and MMNCFs, only $CeSc_2N@C_{80}$[4] and $CeLu_2N@C_{80}$[16] have been successfully studied by ^{13}C NMR. Besides, the ^{45}Sc NMR exhibited a temperature-dependent chemical shift for $CeSc_2N@C_{80}$,[4] and the redox behaviour of $CeLu_2N@C_{80}$ in the anodic range revealed that the removal of the Ce 4f-electron was fulfilled bypassing the carbon cage.[4] To gain a further insight into the nature of influence of the different entrapped metals with more than one 4f-electron, it is still imperative to do the NMR study of MMNCFs which would be the key to open up additional opportunities for the studies of their magnetic properties and cluster-cage interactions.

In this paper, we report the synthesis, isolation and spectroscopic characterization of $Ho_xSc_{3-x}N@C_{80}$ (I, II; x=1, 2). Sc and Ho are chosen as the components of the mixed metal nitride cluster, $Ho_xSc_{3-x}N$, because: a) Sc-based MMNCFs are known to have a relatively higher yield compared to that of the homogeneous NCFs with other lanthanides; b) the radii of their trivalent ions are sufficiently different to study the influence of the different cluster size and the geometry on the cluster-cage interaction; c) the knowledge about dependence of the (para)magnetic behaviour of NCFs comprising lanthanides with more than single 4f-electron is still scarce. To the best of our knowledge, this work is the first investigation of the ^{13}C NMR spectra of $M_2ScN@C_{80}$ (I, M= Lanthanide, except for Lutetium), and ^{45}Sc NMR spectra for the D_{5h} isomer of $MSc_2N@C_{80}$, which was significantly complicated by the relative low-yield (compared to the I_h isomer) and the time-

[a] Y. Zhang, Dr. A. A. Popov, S. Schiemenz, Prof. Dr. L. Dunsch
Group of Electrochemistry and Conducting Polymers
Leibniz-Institute for Solid State and Materials Research (IFW) Dresden
Address 101171 Dresden (Germany)
Fax: (+49) 351-4659-745
E-mail: l.dunsch@ifw-dresden.de

Supporting information for this article is available on the WWW under http://www.chemeurj.org/ or from the author.

consuming multi-steps isolation necessary to obtain the studied compounds in isomerically pure form.

Results and Discussion

Synthesis and isolation of the $Ho_xSc_{3-x}N@C_{80}$ (I, II; x=1, 2) MMNCFs: $Ho_xSc_{3-x}N@C_{80}$ MMNCFs were synthesized by the "reactive gas atmosphere" method as previously described.[8, 12] Figure 1 displays a typical HPLC chromatogram of the $Ho_xSc_{3-x}N@C_{80}$ (I, II; x=1, 2) fullerene extract obtained under the optimized condition (molar ratio Ho/Sc/C=1:1:15). Analyzed by the integrated areas of the corresponding chromatographic peaks, the dominant products are two isomers of $Ho_xSc_{3-x}N@C_{80}$ (x=1, 2), and the relative yield of $Sc_3N@C_{80}$ (I and II) is around 20%.

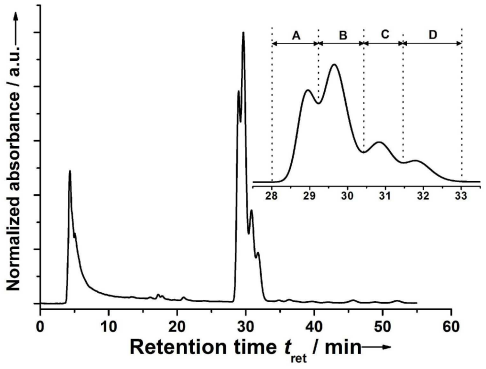

Figure 1. Chromatogram of a raw $Ho_xSc_{3-x}N@C_{2n}$ fullerenes extract synthesized by the "reactive gas atmosphere" method (linear combination of two 4.6×250 mm Buckyprep columns, flow rate 1.6 ml/min, injection volume 200 μL, toluene as mobile phase, 40 ℃). The inset shows the enlarged chromatographic region of 28-33 min.

Two isomers of $Ho_xSc_{3-x}N@C_{80}$ (x=1, 2) were isolated by the multi-step HPLC (see Figures 1, 2). At the first step, linear combination of two 4.6×250 mm Buckyprep columns was used to separate fractions A-D (Figure 1). Each of the fractions was then subjected to the isolation by recycling HPLC on a Buckyprep and/or Buckycluster column (see Supporting Information S1). In particular, to isolate $Ho_2ScN@C_{80}$ (I) from fraction A, first, the Buckyprep column was employed to remove the $HoSc_2N@C_{80}$ (I); second, the Buckycluster column was employed to remove $Sc_3N@C_{78}$ and $HoSc_2N@C_{78}$; third, due to the close retention times of the $Ho_3N@C_{80}$ and $Ho_2ScN@C_{80}$, only small amount of pure $Ho_2ScN@C_{80}$ (I) was obtained by recycling HPLC after 11 cycles (Figure 2a). The isolation of $HoSc_2N@C_{80}$ (I) was achieved after recycling fraction B 10 times to remove the minor components $Sc_3N@C_{78}$, $HoSc_2N@C_{78}$ and $Ho_2ScN@C_{80}$ (I) (Figure 2b). The isolation of $Ho_2ScN@C_{80}$ (II) from the fraction C was accomplished by collecting the fraction between $HoSc_2N@C_{80}$ (I) and $Sc_3N@C_{80}$ (I) after several recycles (Figure 2c). Retention times of $HoSc_2N@C_{80}$ (II) and $Sc_3N@C_{80}$ (II) are quite close; moreover, the amount of these two compounds is quite low in the fraction D. So the mixture of these two compounds had to be enriched in the first step (see Supporting Information S1), then after 24 cycles, limited amount of the purified $HoSc_2N@C_{80}$ (II) could be obtained (Figure 2d). Extended details of the separation of the four compounds can be found in the Supporting Information S1.

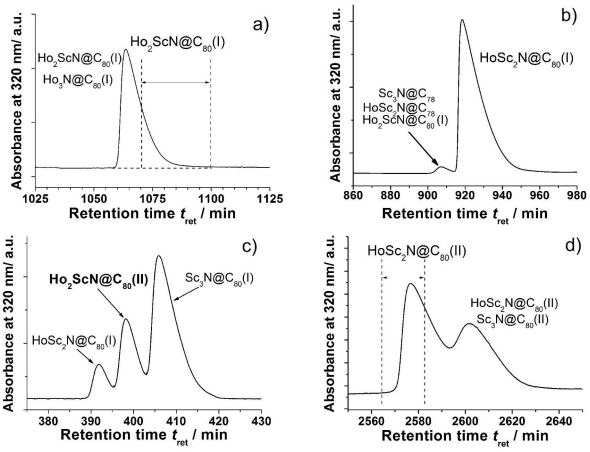

Figure 2. The final isolation steps of $Ho_xSc_{3-x}N@C_{80}$ (I, II; x=1, 2) by recycling HPLC. (a) $Ho_2Sc@C_{80}$ (I), (b) $HoSc_2N@C_{80}$ (I), (c) $Ho_2ScN@C_{80}$ (II) and (d) $HoSc_2N@C_{80}$ (II). (10×250 mm Buckyprep column; flow rate 1.5 ml/min; injection volume 5 ml; toluene as eluent; 20 ℃).

The isolated samples of $Ho_xSc_{3-x}N@C_{80}$ (I, II; x=1, 2) were identified by laser-desorption time-of-flight (LD-TOF) mass spectrum analysis (Figure 3), which confirmed their high purity.

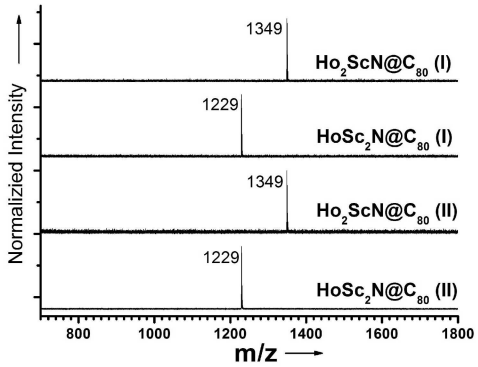

Figure 3. Positive Ion LD-TOF mass spectra of the isolated $Ho_xSc_{3-x}N@C_{80}$ (I, II; x= 1, 2).

Electronic absorption spectra of $Ho_xSc_{3-x}N@C_{80}$ (I, II; x= 0-3): The absorptions of nitride cluster fullerenes in the visible and near-IR range are predominantly due to the π-π* excitations of the carbon cage, which is directly dependent on the structure and the charge state of the carbon cage. A comparison of the spectra of $Ho_xSc_{3-x}N@C_{80}$ (I, II; x=1, 2) in toluene is illustrated in the Figure 4. The electronic absorption spectra of $Ho_xSc_{3-x}N@C_{80}$ (I, x=1, 2), exhibited intermediate spectral features in comparison with $Ho_3N@C_{80}$ (I) and $Sc_3N@C_{80}$ (I) (Figure 4a). $Ho_2ScN@C_{80}$ (I) has mainly inherited the characteristic absorption features of $Ho_3N@C_{80}$ (I) with absorption maxima at 667/696 nm, which are slightly red-shifted to 669/698 nm in $Ho_2ScN@C_{80}$ (I). Substituting the cluster Ho_2ScN for $HoSc_2N$ led to the further red shift of this doublet to 679/713 nm. In addition, the distinct visible absorption peak observed at 399 nm of $Ho_3N@C_{80}$ (I) is shifted to 408 nm in the $Ho_2ScN@C_{80}$ (I) and disappeared in $HoSc_2N@C_{80}$ (I) and $Sc_3N@C_{80}$ (I). Similarly, the shoulder peak of $Ho_3N@C_{80}$ (I) at 557 nm and $HoSc_2N@C_{80}$ (I) at 562 nm gradually faded out in $HoSc_2N@C_{80}$ (I) and $Sc_3N@C_{80}$ (I).

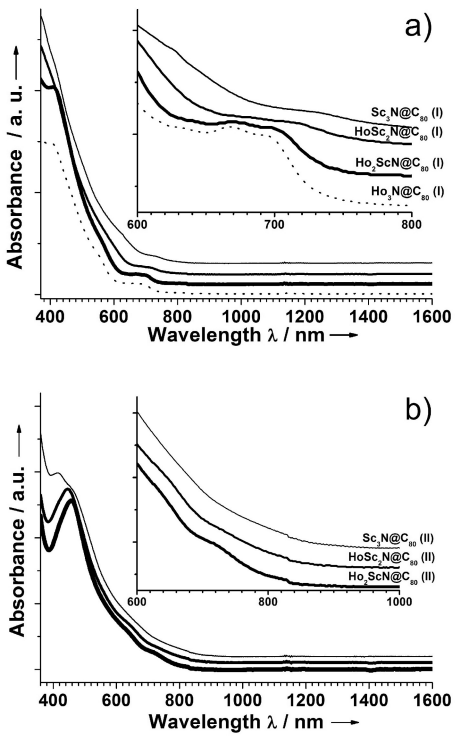

Figure 4. UV-vis-NIR spectra of (a) $Ho_xSc_{3-x}N@C_{80}$ (I; x= 0–3) and (b) $Ho_xSc_{3-x}N@C_{80}$ (II; x= 0–2) in toluene.

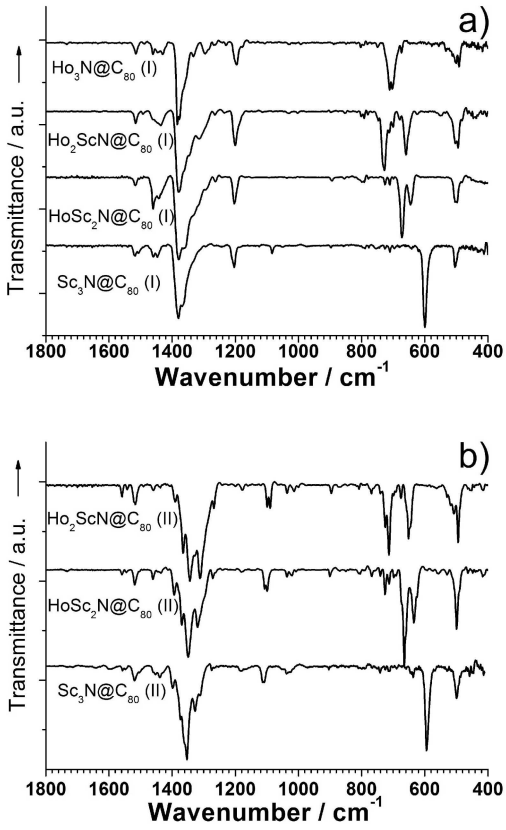

Figure 5. FTIR spectra of (a) $Ho_xSc_{3-x}N@C_{80}$ (I; x= 0–3) and (b) $Ho_xSc_{3-x}N@C_{80}$ (II; x= 0–2).

The electronic absorption spectra of $Ho_xSc_{3-x}N@C_{80}$ (II, x=0–2) are consistent with the differences in the absorption spectra of isomers II found for other MMNCFs.[11] Correspondingly, the absorption peak at 712 nm located in the spectrum of $Ho_2ScN@C_{80}$ (II) is red-shifted to 723 nm for $HoSc_2N@C_{80}$ (II), and vanished in $Sc_3N@C_{80}$ (II). The shoulder peak at 632 nm in the spectrum of $Ho_2ScN@C_{80}$ (II) retained in $HoSc_2N@C_{80}$ (II). Similarly to the isomer I, the strongest absorption peak in the visible range of $Ho_2ScN@C_{80}$ (II) at 457 nm is slightly shifted to 447 nm in the spectrum of $HoSc_2N@C_{80}$ (II) and split into a doublet peak with absorption maxima at 413/472 nm for $Sc_3N@C_{80}$ (II). In summary, electronic absorption features of $HoSc_2N@C_{80}$ (II) exhibit an intermediate state in comparison with $Ho_2ScN@C_{80}$ (II) and $Sc_3N@C_{80}$ (II). The similarities and differences in the overall absorption spectrum of $Ho_xSc_{3-x}N@C_{80}$ (I, II; x=1, 2) are quite close to those of $Gd_xSc_{3-x}N@C_{80}$ (I, II; x=1, 2).[11, 12]

FTIR Vibrational Spectra of $Ho_xSc_{3-x}N@C_{80}$ (I, II; x= 1, 2): Vibrational spectroscopy is a useful tool to analyze the structure of fullerenes due to its high structural sensitivity and its higher time resolution which compared to NMR spectroscopy. The FTIR spectra of $Ho_xSc_{3-x}N@C_{80}$ (I, II; x= 0–3), which are compared in Figure 5, clearly show a similarity of the tangential cage modes (800–1600 cm^{-1}) and radial cage modes (400–600 cm^{-1}) within each groups of MMNCFs with the same cage isomer. The spectra of the MMNCFs (isomer I) are also virtually identical to those of other $M_3N@C_{80}$ (I, M= Sc, Y, Gd, Tb, Dy, Ho, Er, Tm).[20] This result enables us to assign the same cage isomer, C_{80}-I_h(7), to all structures with isomer I. Likewise, cage modes in the spectra of $Ho_xSc_{3-x}N@C_{80}$ (II; x= 1, 2) are very similar to those of $Gd_xSc_{3-x}N@C_{80}$ (II; x= 1, 2) and $Lu_xSc_{3-x}N@C_{80}$ (II; x= 1, 2) with D_{5h}(6) carbon cage.[5, 11]

Figure 5 displays that the antisymmetric metal-nitrogen stretching vibrational modes of $Ho_xSc_{3-x}N@C_{80}$ (I, II; x= 0–3), which are assigned to the most intense low-energy IR lines in the 600–800 cm^{-1} range, are sensitively dependent on the composition of the encaged $Ho_xSc_{3-x}N$ cluster. For $Ho_xSc_{3-x}N@C_{80}$ (I; x= 0–3), the anti-symmetric M–N stretching vibrational mode (ν_{M-N}), which is two-fold degenerate for a homogeneous cluster (at 599 cm^{-1} in $Sc_3N@C_{80}$ (I) and around 710 cm^{-1} in $Ho_3N@C_{80}$ (I)),[20] was found to be split for the $Ho_xSc_{3-x}N$ clusters (645 and 673 cm^{-1} for $HoSc_2N@C_{80}$, 660 and 728 cm^{-1} for $Ho_2ScN@C_{80}$) (Figure 5a). Our recent reports on the analysis of vibrational spectra of the MMNCFs combined with DFT calculations shown that the geometry parameters of the nitride cluster are strongly influenced by the ionic radii of the metal atoms.[5, 11, 12] In particular, an inherent strain of all non-Sc $M_3N@C_{80}$ caused by the limited space inside the carbon cage become appreciably released when the metal atoms is replaced by one or two Sc atoms with smaller ionic radius.[21] As a result, substitution of Ho atoms by Sc results in the synchronous elongation of the Ho-N bonds and shortening of the Sc-N bonds (in comparison to $Ho_3N@C_{80}$ and $Sc_3N@C_{80}$). With the variation of the cluster composition, the ν_{Sc-N} shifts from 599 cm^{-1} in $Sc_3N@C_{80}$ (I) to 673 cm^{-1} in $HoSc_2N@C_{80}$ (I) and to 728 cm^{-1} in $Ho_2ScN@C_{80}$ (I). When the Sc_3N cluster is replaced by the $Ho_xSc_{3-x}N$ cluster within C_{80}-D_{5h}, the M–N stretching vibrational modes experience a similar splitting (see Figure 5b).

A comparison of the FTIR spectra of the isomer I and II of $M_xSc_{3-x}N@C_{80}$ (M= Gd, Dy, Ho, Lu; x=1, 2) is presented in the supporting information S2. As stated, ν_{M-N} is generally split in $M_xSc_{3-x}N@C_{80}$ (x=1, 2), the high-frequency vibrational mode has been definitively assigned to ν_{Sc-N}. By considering the difference of metal radius between Ho^{3+} (Ho^{3+}: 0.90 Å) and other M^{3+} (Gd^{3+}: 0.94Å, Dy^{3+}: 0.91Å, Lu^{3+}: 0.85Å, and Sc^{3+}: 0.75Å),[22] our results

agree well with the studies of $Gd_xSc_{3-x}N@C_{80}$ (I) and $Dy_xSc_{3-x}N@C_{80}$ (I), and $Lu_xSc_{3-x}N@C_{80}$ (I).[5, 11] The shifts for HoScN MMNCFs are smaller than for MMNCFs with larger ions. For $M_2ScN@C_{80}$ (I), $\nu_{Sc\text{-}N}$ increases from 599 cm^{-1} in $Sc_3N@C_{80}$ (I) to 710 cm^{-1} (M = Lu), 728 cm^{-1} (Ho), and further to 737 cm^{-1} (Dy) and 759 cm^{-1} (Gd). In contrast to the $M_2ScN@C_{80}$ (I), the shift in $MSc_2N@C_{80}$ (I) is less pronounced: $\nu_{Sc\text{-}N}$ of $Sc_3N@C_{80}$ (I) (599 cm^{-1}) shifts to 652 cm^{-1} (Lu), 672 cm^{-1} (Ho), 678 cm^{-1} (Dy) and 694 cm^{-1} (Gd). Comparison of the FTIR spectra for the isomer II of $M_xSc_{3-x}N@C_{80}$ (M= Gd, Dy, Ho, and Lu; x= 1, 2) is provided in Supporting Information S2. For $M_2ScN@C_{80}$ (II), $\nu_{Sc\text{-}N}$ increases from 594 cm^{-1} in $Sc_3N@C_{80}$ (II) to 697 cm^{-1} (Lu), 714 cm^{-1} (Ho), 716 cm^{-1} (Dy), and 741 cm^{-1} (Gd). Similar to the $MSc_2N@C_{80}$ (I), the FTIR spectra of $MSc_2N@C_{80}$ (II) demonstrates less pronounced shifts, $\nu_{Sc\text{-}N}$ of $Sc_3N@C_{80}$ (II) (594 cm^{-1}) shifts to 649 cm^{-1} (Lu), 665 cm^{-1} (Ho), 669 cm^{-1} (Dy), and 685 cm^{-1} (Gd). Since the radius of Ho^{3+} is somewhat smaller than that of Gd^{3+} and Dy^{3+}, the fluctuations of $\nu_{Sc\text{–}N}$ induced by encaged Ho atom(s) are less prominent than those for Gd and Dy. Thus, as discussed above, the splitting of $\nu_{Sc\text{–}N}$ is considerably dependent on the composition of the encaged $M_xSc_{3-x}N$ cluster and also exhibits some dependence on the cage symmetry.

Raman spectra of $Ho_xSc_{3-x}N@C_{80}$ (I, II; x= 1, 2). The Raman spectra of nitride cluster fullerenes commonly consist of four regions: the tangential C_{80} modes in the range of 1000–1600 cm^{-1}; a gaplike region from 815 to 1000 cm^{-1}, the radial breathing cage modes between 200 and 815 cm^{-1}, and the low-energy metal cage modes below 200 cm^{-1}. A detailed analysis of low-energy metal cage modes is shown below, which give us more information on the structure of the cluster and cluster-cage interaction.

A comparison of the Raman spectra of $Ho_xSc_{3-x}N@C_{80}$ (I, II; x=0–2) is presented in the Figure 6. Similar to the IR spectra, spectral patterns of the $Ho_xSc_{3-x}N@C_{80}$ MMNCFs with the same carbon cage are rather similar and are considerably different when two cage isomers of the same cluster composition are compared with each other. Some differences in the relative intensity of the Raman bands could be ascribed to the different resonance effects of the specific structures. To investigate the interaction between the $Ho_xSc_{3-x}N$ cluster and the C_{80} cage, the low-energy part of the vibrational pattern in the Raman spectrum was studied as well, due to it is correlation to the bond formation between the nitride cluster and carbon cage. The low-energy part of the Raman spectra of $Ho_xSc_{3-x}N@C_{80}$ (I, II; x=0-2) observed at 120 K with the laser wavelength of 647 nm consisted of the radial C_{80} cage modes and of cluster-based modes ranging from 220 to 40 cm^{-1} (Figure 7). The cluster-based modes included the in-plane cluster deformation mode and the frustrated translations and rotations of the nitride cluster, which provided critical information about the interaction between the entrapped nitride cluster and the C_{80} cage. As showed in our earlier report on the Raman/DFT study on the $Gd_xSc_{3-x}N@C_{80}$, the medium-intensity Raman lines of $Sc_3N@C_{80}$ (I) at 210 cm^{-1} referred to the frustrated in-plane cluster translation with a partial contribution from the in-plane M_3N deformation.[11] In the case of antisymmetric metal-nitrogen stretching vibrational mode of $Ho_xSc_{3-x}N$, the mode of homogeneous Sc_3N cluster is split into two components for the $HoSc_2N$ and Ho_2ScN mixed cluster similar to the anitisymmetric M-N modes in the IR spectra (this mode is also two-degenerate in the homogeneous nitride clusterfullerenes). In the Raman spectrum of the isomer I, two lines at 213/166 cm^{-1} for $HoSc_2N@C_{80}$ and at 178/162 cm^{-1} for $Ho_2ScN@C_{80}$ are assigned to this kind of vibrations. Compared to the isomer I, the subtle shifts of lines for the isomer II of $Ho_xSc_{3-x}N@C_{80}$ could be determined,

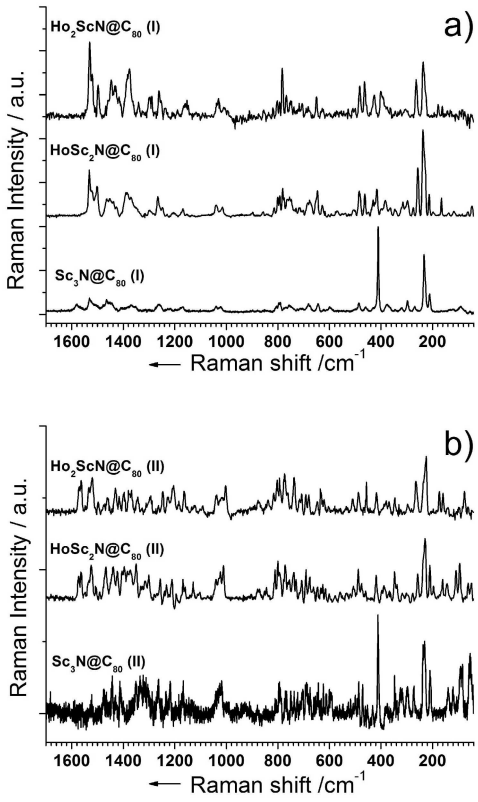

Figure 6. Raman spectra of (a) $Ho_xSc_{3-x}N@C_{80}$ (I; x= 0-2) and (b) $Ho_xSc_{3-x}N@C_{80}$ (II; x= 0–2).

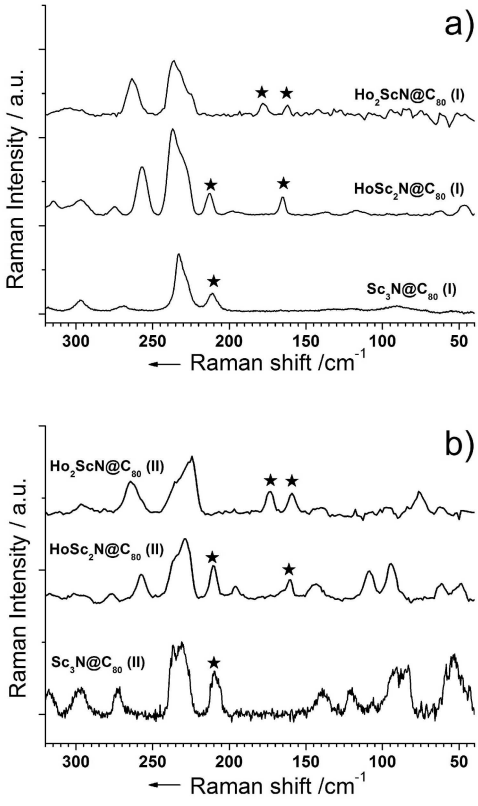

Figure 7. The low-energy Raman spectra of $Ho_xSc_{3-x}N@C_{80}$ (I, II; x= 0–2) were obtained at 120 K and with the laser wavelength of 647 nm. The asterisks mark the in-plane cluster deformation modes (ν_{def}).

211/160 cm^{-1} for the $HoSc_2N@C_{80}$ and 173/159 cm^{-1} for $Ho_2ScN@C_{80}$, due to the alteration of the cage symmetry. Based on experimental and earlier theoretical studies, the difference between the $Gd_xSc_{3-x}N@C_{80}$ and $Ho_xSc_{3-x}N@C_{80}$ (x=1, 2), could be explained by the increasing mass of the metal cluster and the decreasing cluster-cage force constants.[11, 20]

NMR Studies and Assignments of $Ho_xSc_{3-x}N@C_{80}$ (I, II; x= 1, 2): In the present state of the NCFs knowledge, ^{13}C NMR spectra could be regarded as a definitive proof for determining the symmetry of the carbon cage. The studies of Cerium-based MMNCFs ($CeSc_2N@C_{80}$[4] and $CeLu_2N@C_{80}$[16]) showed that even the single 4f-electron on the Ce atom induces considerable paramagnetic chemical shift and broadening of the ^{13}C NMR lines. Similar effects were observed in numerous ^{13}C NMR studies of Ce-based mono- and dimetallofullerenes and their derivatives.[23] To our knowledge, the only paramagnetic ^{13}C NMR studies of non-Ce lanthanide metallofullerenes were reported for three isomers of $Tm@C_{82}$[24] and for the $Pr@C_{82}^-$ anion.[25] The influence of multiple 4f-electrons on the carbon cage is still unresolved question which requires further study.

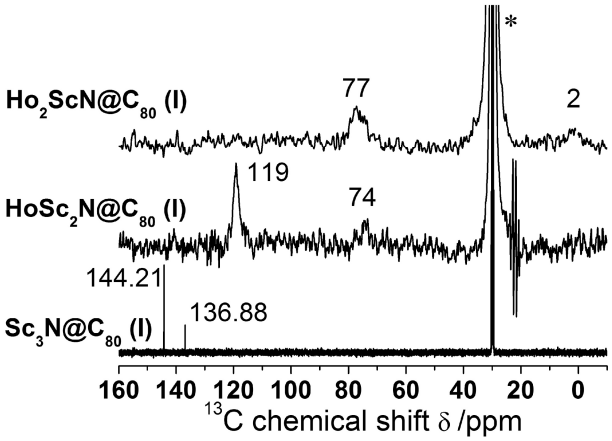

Figure 8. ^{13}C NMR spectra of $Ho_xSc_{3-x}N@C_{80}$ (I, II; x= 0–2) CS_2/d_6-acetone at the room temperature. An asterisk denotes the signal of the solvent.

Herein, we report the first ^{13}C NMR spectroscopy of $Ho_xSc_{3-x}N@C_{80}$ (I; x= 1–2). The 125 MHz ^{13}C NMR spectra of $Ho_xSc_{3-x}N@C_{80}$ (I; x= 1–2) obtained at room temperature exhibit two broad peaks with chemical shift of 119 and 74 ppm ($HoSc_2N@C_{80}$), and 77 and 2 ppm ($Ho_2ScN@C_{80}$), respectively (Figure 8). The intensity ratio of these two lines is roughly 3:1, which is characteristic for classical NCF with the C_{80} (I_h) cage isomer. Thus, paramagnetic shift of the ^{13}C NMR lines induced by each Sc-to-Ho substitution is 25–40 ppm for the more intense peak and 60–70 ppm for the second peak. For comparison, the shift of the ^{13}C lines in $CeM_2N@C_{80}$ (M = Sc, Lu) in comparison to $Sc_3N@C_{80}$ the did not exceed 2 ppm. Such a large difference in the lanthanide-induced shift obviously originates form the much higher effective magnetic moment of $4f^{10}$-Ho^{3+} (10.6 μ_B) than $4f^1$-Ce^{3+} (2.54 μ_B). A complete interpretation of the paramagnetic chemical shift can be achieved only by the combination of two factors, local instantaneous paramagnetic shifts of carbon atoms induced by Ho^{3+} and the internal motion of the encapsulated nitride cluster which averages these interactions on the NMR time scale. Complete analysis of these factors will be presented elsewhere.

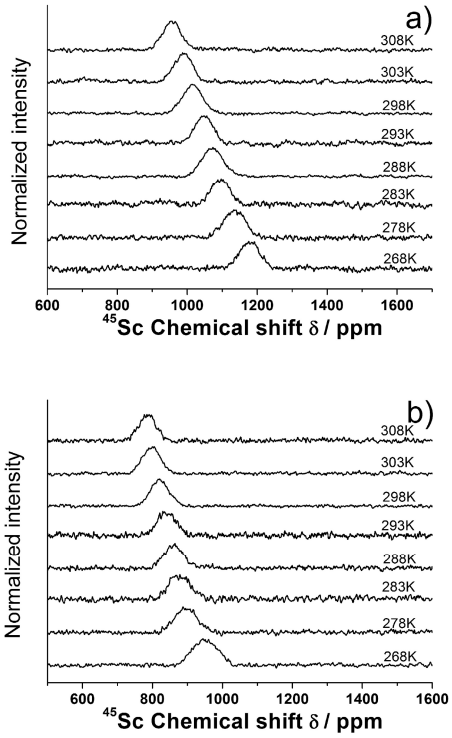

Figure 9. ^{45}Sc NMR spectra of $HoSc_2N@C_{80}$ (I, a) and (II, b) measured at the different temperature.

Large temperature-dependent paramagnetic shifts were also observed in the ^{45}Sc NMR spectra of $HoSc_2N@C_{80}$ (I, II) shown in Fig. 9. In the temperature range from 268 K to 308 K in the CS_2 solution, both compounds exhibited single peak ^{45}Sc NMR peak, showing that two Sc atoms are averaged by the cluster dynamics. In comparison to the ^{45}Sc signals in $Sc_3N@C_{80}$ (δ = 199.5 ppm for I_h and 211.7 ppm for D_{5h} isomers), ^{45}Sc chemical shifts of $HoSc_2N@C_{80}$ are shifted donwfield by ca 900 ppm for the I_h-cage (δ = 1178-956 ppm) and 700 ppm for the D_{5h}-cage (δ = 950-786 ppm), while the line is ca 1.5 times broader (note that the ^{45}Sc lines are intrinsically broadened because of the quadruple moment of Sc). Importantly, for the same compound, paramagnetic shift of the ^{45}Sc signal is much higher than that in the ^{13}C NMR spectrum, which can be explained by a dynamic nature of the ^{13}C NMR. In ^{13}C NMR, the measured signal is averaged for all carbon atoms of a given type (and hence it has contribution both from the atoms which are far away from the Ho ion and have small instant paramagnetic contribution and from those which are close to Ho). On the contrary, the $HoSc_2N$ cluster has rigid geometry with constant Sc–Ho distances. As a result, ^{45}Sc NMR is a more sensitive probe of the paramagnetic effect of Ho atom.

The main contributions to paramagnetic chemical shifts in solution are Fermi contact (δ_{fc}) and pseudo-contact (δ_{pc}) shifts, which scale with temperature as T^{-1} and T^{-2} (here T is absolute temperature), respectively. For Ce-based mono- or dimetallofullerenes and MMNCFs, the temperature-dependent NMR studies revealed that the contact term δ_{fc} is negligible, and the chemical shift can be simply expressed as $\delta = \delta_{dia} + c_{pc}\cdot T^{-2}$.[4, 16, 23] For $HoSc_2N@C_{80}$, the diamagnetic term (δ_{dia}) can be estimated by extrapolating δ dependence to T^{-2}=0, while the c_{pc} is determined as an increment of the linear dependence δ vs T^{-2}. If the assumption that pseudocontact shift is the dominant term is correct, δ_{dia} should be close to the ^{45}Sc chemical shift of $Sc_3N@C_{80}$ isomers (δ =

200−212 ppm). For both isomers, extrapolation to T^{-2}=0 yielded δ_{dia} = 271 ppm. For comparison, extrapolation to T^{-1}=0 gave δ_{dia} values of −531 and −319 ppm for I_h and D_{5h} isomers, respectively, which is substantially further from the $Sc_3N@C_{80}$ value. Thus, the prevalence of the pseudocontact term is confirmed for $HoSc_2N@C_{80}$. At the same time, the difference between extrapolated δ_{dia} values and experimental value for $Sc_3N@C_{80}$ is rather large which indicates that the contact term is probably not negligible. Precise estimation of the contact term contribution to lanthanide paramagnetic shift is not possible at this moment and requires a study of a series of $MSc_2N@C_{80}$ MMNCFs with different lanthanides,[26] which is underway in our group.

Interestingly, although δ_{dia} values for the two isomers of $HoSc_2N@C_{80}$ are identical, their c_{pc} values determined from the linear fitting of experimental data by the $\delta_{dia} + c_{pc}\cdot T^{-2}$ function are substantially different: for the I_h isomer, the fitting gives c_{pc} = 66±3 ppm·K^2, while c_{pc} of the D_{5h} isomer is found to be 49±0.5 ppm·K^2. The reason for such a significant variation is not clear at this moment; possibly, the difference of c_{pc} constants partially reflects the difference in the geometrical structure of the $HoSc_2N$ cluster inside different carbon cages (note that c_{pc} scales with the distance R between paramagnetic center and the atom of interest as R^{-3}).[27] FTIR spectroscopy (see above) showed that the frequencies of the metal-nitrogen modes in $HoSc_2N@C_{80}$ (II) are ca 10 cm^{-1} lower than in $HoSc_2N@C_{80}$ (I), which means that corresponding bond lengths in the D_{5h} isomer are somewhat longer.[21] Besides, single-crystal X-ray studies of $M_3N@C_{80}$-D_{5h} (M = Sc, Tb, Tm) also show that the nitride cluster inside the C_{80}-D_{5h} cage tends to be somewhat more distorted from the trigonal symmetry than in the I_h isomers.[28] In addition to the geometrical changes, distortion of the cluster may also change the crystal-field splitting parameters and hence also affect the c_{pc} values. Detailed analysis of these factors exceeds the scope of this paper and will be reported elsewhere.

It is also instructive to compare pseudocontact shifts in MMNCFs with different lanthanides. Variable-temperature ^{45}Sc chemical shifts of $CeSc_2N@C_{80}$-I_h reported by Dorn *et al.*[4] give c_{pc} of 6.6 ppm·K^2, which is an order of magnitude smaller than found in this work for $HoSc_2N@C_{80}$-I_h. A ten-fold increase of the c_{pc} value for $HoSc_2N@C_{80}$ is reasonable taking into account a higher magnetic moment of Ho^{3+} when compared to that of Ce^{3+}. In particular, in the framework of Bleaney theory, if the difference in geometrical and crystal-field parameters for $CeSc_2N@C_{80}$ and $HoSc_2N@C_{80}$ are neglected, the ratio of pseudocontact shifts induced by Ce^{3+} and Ho^{3+} at room temperature is expected to be −6.3/−39.0,[27] which is close to the experimentally determined ratio of c_{pc} values for ^{45}Sc.

Conclusions

In summary, we have synthesized and isolated the $Ho_xSc_{3-x}N@C_{80}$ (I, II; x=1, 2). A systematic comparison of the UV-Vis-NIR, FTIR and Raman spectroscopic studies indicates that the vibrational modes of $Ho_xSc_{3-x}N@C_{80}$ (x= 1, 2) resemble to $Ho_3N@C_{80}$ and $Sc_3N@C_{80}$. The 4f^{10}-electrons located on the Ho atom results in remarkable broadness of the NMR peaks and strong paramagnetic chemical shifts in the ^{13}C and ^{45}Sc NMR spectra. The variable-temperature ^{45}Sc NMR spectroscopic study demonstrated that Ho-induced paramagnetic shift is dominated by the pseudocontact term. As the first successful and comprehensive report on the ^{13}C and ^{45}Sc NMR with more than one unpaired 4f-electron on the encaged nitride cluster with different cage symmetry, this study shows possibilities for the further studies of the state of paramagnetic metal atoms in the mixed metal nitride clusterfullerenes.

Experimental Section

$Ho_xSc_{3-x}N@C_{80}$ (I, II; x=1, 2) MMNCFs are synthesized by a modified Krätschmer-Huffman dc-arc discharging method with the addition of NH_3 (20 mbar) as described elsewhere. Briefly, a mixture of Ho_2O_3 and Sc_2O_3 (99.9%, MaTeck GmbH, Germany) and graphite powder was used (molar ratio Ho/Sc/C=1:1:15). After dc-arc discharging, the soot was pre-extracted by acetone and further Soxhlet-extracted by CS_2 for 20h. The isolation of Ho-based MMNCFs was performed by three-step HPLC. The first step running in a Hewlett-Packard instrument (series 1100), a linear combination of two analytical 4.6×250 mm Buckyprep columns (Nacalai Tesque, Japan) was applied with toluene as the eluent. The second- and third-step isolation were performed by a recycling HPLC (Sunchrom, Germany) using a Buckyprep columns or Buckycluster column (Nacalai Tesque, Japan) and toluene as the eluent. The UV detector set to 320 nm was employed for fullerene detection for all steps. The purity of the isolated products was checked by laser desorption time-of-flight (LD-TOF) MS analysis running in both and positive and negative ion modes (Biflex III, Bruker, Germany). Sample preparation and experimental details for UV/Vis/NIR, FTIR and Raman spectroscopic measurements have been described previously. The 125 MHz ^{13}C NMR and 121.5 MHz ^{45}Sc NMR spectroscopic measurements were performed at in a multiprobe head PH 1152Z on an Avance 500 spectrometer (Bruker, Germany) at room temperature in carbon disulfide solutions with d_6-acetone as a lock.

Acknowledgements

We cordially acknowledge the technical assistance of F. Ziegs and M. Rosenkranz (all at IFW Dresden). This work was supported by DFG (project PO 1602/1-1 to A.A.P.) and a fellowship from Chinese Scholar Council (to Y. Zh.).

[1] S. Stevenson, G. Rice, T. Glass, K. Harich, F. Cromer, M. R. Jordan, J. Craft, E. Hadju, R. Bible, M. M. Olmstead, K. Maitra, A. J. Fisher, A. L. Balch, H. C. Dorn, *Nature* **1999**, *401*, 55-57.

[2] S. Yang, C. Chen, A. Popov, W. Zhang, F. Liu, L. Dunsch, *Chem. Commun.* **2009**, 6391-6393.

[3] N. Chen, L. Z. Fan, K. Tan, Y. Q. Wu, C. Y. Shu, X. Lu, C. R. Wang, *J. Phys. Chem. C* **2007**, *111*, 11823-11828.

[4] X. L. Wang, T. M. Zuo, M. M. Olmstead, J. C. Duchamp, T. E. Glass, F. Cromer, A. L. Balch, H. C. Dorn, *J. Am. Chem. Soc.* **2006**, *128*, 8884-8889.

[5] S. Yang, A. A. Popov, C. Chen, L. Dunsch, *J. Phys. Chem. C* **2009**, *113*, 7616-7623.

[6] S. Stevenson, C. Chancellor, H. M. Lee, M. H. Olmstead, A. L. Balch, *Inorg. Chem.* **2008**, *47*, 1420-1427.

[7] M. M. Olmstead, A. de Bettencourt-Dias, J. C. Duchamp, S. Stevenson, H. C. Dorn, A. L. Balch, *J. Am. Chem. Soc.* **2000**, *122*, 12220-12226.

[8] L. Dunsch, M. Krause, J. Noack, P. Georgi, *J. Phys. Chem. Solids* **2004**, *65*, 309-315.

[9] R. M. Macfarlane, D. S. Bethune, S. Stevenson, H. C. Dorn, *Chem. Phys. Lett.* **2001**, *343*, 229-234.

[10] N. Chen, E. Y. Zhang, C. R. Wang, *J. Phys. Chem. B* **2006**, *110*, 13322-13325.

[11] S. F. Yang, A. A. Popov, M. Kalbac, L. Dunsch, *Chem.-Eur. J.* **2008**, *14*, 2084-2092.

[12] S. F. Yang, M. Kalbac, A. Popov, L. Dunsch, *ChemPhysChem* **2006**, *7*, 1990-1995.

[13] S. Yang, A. A. Popov, L. Dunsch, *Angew. Chem.-Int. Edit. Engl.* **2008**, *47*, 8196-8200.

[14] S. F. Yang, A. A. Popov, L. Dunsch, *Chem. Commun.* **2008**, 2885-2887.

[15] S. Yang, A. A. Popov, L. Dunsch, *J. Phys. Chem. B* **2007**, *111*, 13659-13663.

[16] L. Zhang, A. A. Popov, S. Yang, S. Klod, P. Rapta, L. Dunsch, *Phys. Chem. Chem. Phys.* **2010**, *12*, 7840-7847.

[17] R. M. Macfarlane, D. S. Bethune, S. Stevenson, H. C. Dorn, *Chemical Physics Letters* **2001**, *343*, 229-234; J. G. M. Morton, A. Tiwari, G. Dantelle, K. Porfyrakis, A. Ardavan, G. A. D. Briggs, *Phys. Rev. Lett.* **2008**, *101*, 013002; A. Tiwari, G. Dantelle, K. Porfyrakis, A. Ardavan, G. A. D. Briggs, *physica status solidi (b)* **2008**, *245*, 1998-2001.

[18] A. Tiwari, G. Dantelle, K. Porfyrakis, A. A. R. Watt, A. Ardavan, G. A. D. Briggs, *Chem. Phys. Lett.* **2008**, *466*, 155-158.

[19] W. Fu, J. Zhang, H. Champion, T. Fuhrer, H. Azuremendi, T. Zuo, J. Zhang, K. Harich, H. C. Dorn, *Inorg. Chem.* **2011**, *50*, 4256-4259; W. Fu, L. Xu, H. Azurmendi, J. Ge, T. Fuhrer, T. Zuo, J. Reid, C. Shu, K. Harich, H. C. Dorn, *J. Am. Chem. Soc.* **2009**, *131*, 11762-11769; S. Stevenson, P. W. Fowler, T. Heine, J. C. Duchamp, G. Rice, T. Glass, K. Harich, E. Hajdu, R. Bible, H. C. Dorn, *Nature* **2000**, *408*, 427-428; J. C. Duchamp, A. Demortier, K. R. Fletcher, D. Dorn, E. B. Iezzi, T. Glass, H. C. Dorn, *Chem. Phys. Lett.* **2003**, *375*, 655-659.

[20] S. F. Yang, S. I. Troyanov, A. A. Popov, M. Krause, L. Dunsch, *J. Am. Chem. Soc.* **2006**, *128*, 16733-16739.

[21] A. A. Popov, *J. Comput. Theor. Nanosci.* **2009**, *6*, 292-317.

[22] N. N. Greenwood, A. Earnshaw, *Chemistry of the Elements*, Pergamon, Oxford, **1984**.

[23] Y. Takano, M. Aoyagi, M. Yamada, H. Nikawa, Z. Slanina, N. Mizorogi, M. O. Ishitsuka, T. Tsuchiya, Y. Maeda, T. Akasaka, T. Kato, S. Nagase, *J. Am. Chem. Soc.* **2009**, *131*, 9340-9346; M. Yamada, N. Mizorogi, T. Tsuchiya, T. Akasaka, S. Nagase, *Chem.-Eur. J.* **2009**, *15*, 9486-9493; M. Yamada, T. Wakahara, T. Tsuchiya, Y. Maeda, M. Kako, T. Akasaka, K. Yoza, E. Horn, N. Mizorogi, S. Nagase, *Chem. Commun.* **2008**, 558-560; M. Yamada, C. Someya, T. Wakahara, T. Tsuchiya, Y. Maeda, T. Akasaka, K. Yoza, E. Horn, M. T. H. Liu, N. Mizorogi, S. Nagase, *J. Am. Chem. Soc.* **2008**, *130*, 1171-1176; M. Yamada, T. Wakahara, T. Tsuchiya, Y. Maeda, T. Akasaka, N. Mizorogi, S. Nagase, *J. Phys. Chem. A* **2008**, *112*, 7627-7631; M. Yamada, T. Wakahara, Y. Lian, T. Tsuchiya, T. Akasaka, M. Waelchli, N. Mizorogi, S. Nagase, K. M. Kadish, *J. Am. Chem. Soc.* **2006**, *128*, 1400-1401.

[24] T. Kodama, N. Ozawa, Y. Miyake, K. Sakaguchi, H. Nishikawa, I. Ikemoto, K. Kikuchi, Y. Achiba, *J. Am. Chem. Soc.* **2002**, *124*, 1452-1455.

[25] T. Wakahara, S. Okubo, M. Kondo, Y. Maeda, T. Akasaka, M. Waelchli, M. Kako, K. Kobayashi, S. Nagase, T. Kato, K. Yamamoto, X. Gao, E. Van Caemelbecke, K. M. Kadish, *Chem. Phys. Lett.* **2002**, *360*, 235-239.

[26] S. D. Pietro, S. L. Piano, L. D. Bari, *Coord. Chem. Rev.* **2011**, *255*, 2810-2820; C. N. Reilley, B. W. Good, J. F. Desreux, *Anal. Chem.* **1975**, *47*, 2110-2116.

[27] B. Bleaney, *J. Magn. Reson.* **1972**, *8*, 91-100; B. Bleaney, C. M. Dobson, B. A. Levine, R. B. Martin, R. J. P. Williams, A. V. Xavier, *J. Chem. Soc., Chem. Commun.* **1972**, 791-793.

[28] T. Zuo, M. M. Olmstead, C. M. Beavers, A. L. Balch, G. Wang, G. T. Yee, C. Shu, L. Xu, B. Elliott, L. Echegoyen, J. C. Duchamp, H. C. Dorn, *Inorg. Chem.* **2008**, *47*, 5234-5244; T. M. Zuo, C. M. Beavers, J. C. Duchamp, A. Campbell, H. C. Dorn, M. M. Olmstead, A. L. Balch, *J. Am. Chem. Soc.* **2007**, *129*, 2035-2043; T. Cai, L. S. Xu, M. R. Anderson, Z. X. Ge, T. M. Zuo, X. L. Wang, M. M. Olmstead, A. L. Balch, H. W. Gibson, H. C. Dorn, *J. Am. Chem. Soc.* **2006**, *128*, 8581-8589.

Received: ((will be filled in by the editorial staff))
Revised: ((will be filled in by the editorial staff))
Published online: ((will be filled in by the editorial staff))

Entry for the Table of Contents

Ho-induced ^{13}C and ^{45}Sc NMR shift

*Yang Zhang, Alexey A Popov, Sandra Schiemenz, and Lothar Dunsch**……..…… Page – Page

Synthesis, Isolation and Spectroscopic Characterization of Holmium-Based Mixed Metal Nitride Clusterfullerenes: $Ho_xSc_{3-x}N@C_{80}$ (x=1, 2)

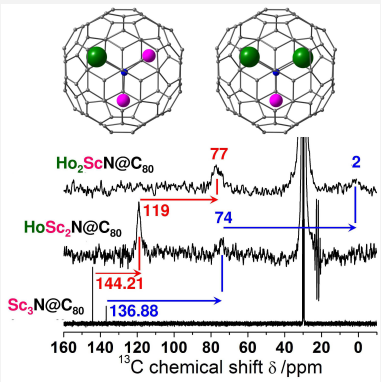

$Ho_xSc_{3-x}N@C_{80}$ (x=1, 2) nitride clusterfullerenes with $I_h(7)$ and $D_{5h}(6)$ are synthesized and isolated, and their characterization by ^{13}C and ^{45}Sc VT-NMR spectroscopy is accomplished for first time for any Ho-based endohedral fullerene. Analysis of the Ho-induced the paramagnetic shifts reveals the influence of the paramagnetic lanthanide ion on its surroundings